



Original Article

2D Shear Wave Imaging in Gaussian Noise and Reflection Media

Tran Quang Huy¹, Pham Thi Thu Ha^{2,3}, Tran Binh Duong^{4,5},
Nguyen Quang Vinh², Nguyen Thi Hoang Yen⁶, Tran Duc Tan^{7,*}

¹Hanoi Pedagogical University 2, 32 Nguyen Van Linh, Xuan Hoa, Phuc Yen, Vinh Phuc, Vietnam

²Vietnam Academy of Military Science and Technology, 17 Hoang Sam, Cau Giay, Hanoi, Vietnam

³Hanoi-Amsterdam High School for the Gifted, 1 Hoang Minh Giam, Cau Giay, Hanoi, Vietnam

⁴School of Information Science and Engineering, Southeast University,
2 Sipai Building, Xuanwu District, Nanjing, China

⁵Vietnam Paper Corporation, 25A Ly Thuong Kiet, Hoan Kiem, Hanoi, Vietnam

⁶National University of Education, 136 Xuan Thuy, Cau Giay, Hanoi, Vietnam

⁷Phenikaa University, 1 Nguyen Van Trac, Yen Nghia, Ha Dong, Hanoi, Vietnam

Received 31 January 2021

Revised 14 March 2021; Accepted 14 March 2021

Abstract: Shear wave imaging (SWI) is a rapid and convenient method of collecting images of tissues in the region of interest. SWI is based on the mechanical properties of soft tissues named the complex shear modulus (CSM). The complex shear modulus consisting of the elasticity and the viscosity, is useful for diagnosing pathological tissue conditions. Previous studies have not fully exploited the estimation of CSM in the medium containing Gaussian noise and the shear wave's reflection phenomenon. In this study, we focused on the model of shear wave propagation in the 2D environment by the time domain finite difference method (FDTD), taking into account the effect of Gaussian noise and reflected shear wave. We then reduced the noise of the measured particle velocity using a designed least mean square filter. Finally, for direct estimation of CSM, Helmholtz algebraic inverse transformation algorithm was used. Reflected waves significantly affect the estimation of CSM, especially the tissue's viscosity, which is demonstrated by numerical simulation results.

Keywords: Shear wave, CSM, Gaussian noise, reflection, FDTD.

* Corresponding author.

E-mail address: tan.tranduc@phenikaa-uni.edu.vn

<https://doi.org/10.25073/2588-1124/vnumap.4631>

1. Introduction

Many scientific studies have shown that 70-80% of liver cancers develop based on cirrhosis, so cirrhosis risk factors are also considered risk factors for HCC. According to medical experts, the diagnosis of cirrhosis is one of the important criteria in deciding on treatment, monitoring disease progression, and prognosis. In diagnosing cirrhosis, liver biopsy is considered the gold standard. However, the biopsy is an invasive method that causes pain and complications such as bleeding, infection, ... In addition, the accuracy of the biopsy sample is also an issue that can lead to deviation in the assessment of cirrhosis. With the development of science and technology, shear wave ultrasound can help doctors diagnose liver fibrosis and the tumor's hardness.

Shear wave ultrasound is a new technique in imaging ultrasound, helping determine the organ's elasticity, damage. This technique is performed as a routine ultrasound on the ultrasonic machine featuring shear wave ultrasound. This ultrasound method enhances the specificity of the diagnosis and helps narrow the biopsy indication without missing lesions. The authors in [1] have mentioned the shear wave elastic imaging (SWEI) technique used in medical diagnosis. Subsequently, the shear wave propagation velocity is related to the elasticity and viscosity of the medium [2] given by the equations of Chen et al. Methods for quantifying tissue elasticity and viscosity through distortion wave velocity measurements were proposed shortly thereafter. The authors also used the filter MLEF (Maximum Likelihood Ensemble Filter) to estimate the CSM parameter for a homogeneous environment based on the Kelvin-Voigt model [3]. Research on CSM (Complex Shear Modulus) estimation and shear wave ultrasound imaging to date is still attracting significant interest from different research groups [4-12]. However, the shear wave ultrasonic imaging process is always influenced by Gaussian noise, and the reflection phenomenon reduces the estimated image quality. Therefore, in this paper, we study the problem of estimating two-dimensional complex shear modulus (2D-CSM) in the medium containing Gaussian noise, and the reflection phenomenon of shear waves appears. Quantitative information about the tissue's elasticity and viscosity to help the doctors make a more accurate diagnosis is the intended outcome of the paper.

2. Methodology

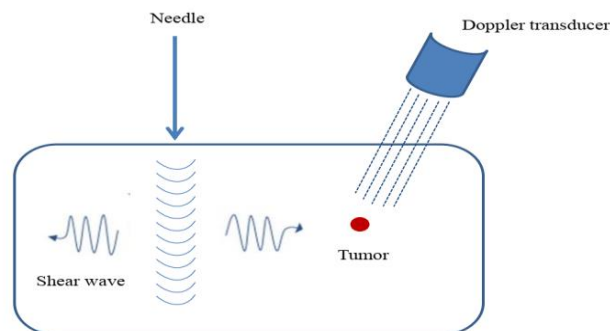


Figure 1. Excitation and shear wave measurement system.

A needle is vibrated at a specified frequency along the Z-axis in the elastic ultrasonic imaging system, which then propagates across the X-Y plane (Figure 1). Such particle velocities can be collected using Doppler ultrasound [3].

Therefore, assuming no absorbing medium, the propagation of shear wave sliding along the radial axis, the FDTD method is used. The particle velocity vector v_z in the direction of propagation of the x-wave in the Cartesian coordinate system and the compressed tensor σ_{zx} have the relationship expressed by equations (1) and (2) [7]:

$$\rho \partial_t v_z = \partial_x \sigma_{zx}, \quad (1)$$

$$\partial_t \sigma_{zx} = (\mu + \eta \partial_t) \partial_x v_z, \quad (2)$$

where ∂_t and ∂_x respectively are separate derivative operators of ∂/∂_t and ∂/∂_x applied for the value to the right of the symbol; ρ , μ and η are denoting represented tissue density, elasticity, and viscosity, respectively. The Kelvin-Voigt model represents complex strain modulus CSM $G(x, \omega)$; this quantity depends on angular frequency ω as follows:

$$G(x, \omega) = \mu(x) - i\omega\eta(x), \quad (3)$$

where μ is the elasticity and viscosity η is to be estimated. The following symbols are used to discrete equations (1) and (2):

$$v_z(x, t) = v_z(i\Delta x, n\Delta t) = v_z^n|_i \quad (4)$$

$$\sigma_{zx}(x, t) = \sigma_{zx}(i\Delta x, n\Delta t) = \sigma_{zx}^n|_i \quad (5)$$

The sampling period, the step-time space step-index are represented as Δt , i , and n , respectively. Using the FDTD method, (1) and (2) are described as follows:

$$v_z^{n+1}|_i = v_z^n|_i + \frac{\Delta t}{\rho\Delta x} \left(\sigma_{zx}^{n+\frac{1}{2}} \Big|_{i+\frac{1}{2}} - \sigma_{zx}^{n+\frac{1}{2}} \Big|_{i-\frac{1}{2}} \right) \quad (6)$$

$$\begin{aligned} \sigma_{zx}^{n+\frac{1}{2}} \Big|_{i+\frac{1}{2}} &= \sigma_{zx}^{n-\frac{1}{2}} \Big|_{i+\frac{1}{2}} + \frac{\mu\Delta t}{\Delta x} (v_z^{n+1}|_{i+1} - v_z^{n+1}|_i) + \frac{\eta}{\Delta x} (v_z^{n+1}|_{i+1} - v_z^{n+1}|_i) \\ &\quad - \frac{\eta}{\Delta x} (v_z^n|_{i+1} - v_z^n|_i), \end{aligned} \quad (7)$$

where $v_z(n)$ represents the particle velocity signal affected by the Gaussian noise transmitted into the tissue, represented as $z(n)$. At the same time, they form the noise signal $v_z(n)$ described by:

$$v(n) = v_z(n) + z(n) \quad (8)$$

The Least Mean Square (LMS) filter's input signal is the noisy signal $v(n)$ aiming to extract the desired signal estimate $v_z(n)$. The signal is filtered $\hat{v}_z(n)$ or the bandpass filter output, sampled and formed a vector with N samples:

$$v(n) = [v_z(0), v_z(1), \dots, v_z(N-1)], \quad (9)$$

and the filter coefficients are expressed as follows:

$$\omega(n) = [\omega(0), \omega(1), \dots, \omega(L)], \quad (10)$$

where L denotes the order of the filter. The $\omega(n)$ is called weighting.

After reducing the noise from the obtained particle velocity, the AHI algorithm [8] was used to compute the CSM. For small volumes, it is assumed that the viscous elastic property of tissue is isotropic. We combine (1) and (2) to obtain:

$$\rho \frac{\partial^2 v_z}{\partial t^2} = G'(x, t) \nabla^2 v_z, \tag{11}$$

where $G'(x, t)$ is CSM in the time domain, and $\nabla^2 v_z$ is the Laplace operator of v_z defined as $\nabla^2 v_z = \frac{\partial^2 v_z}{\partial x^2}$.

To solve (11), the AHI algorithm is applied, which then became the Helmholtz equation:

$$\left(\frac{G(x, \omega)}{\rho} \nabla^2 + \omega^2 \right) V_z(x, \omega) |_{\omega=\omega_0} = 0, \tag{12}$$

where $G(x, \omega)$ is CSM in the frequency domain and defined in (3), $V_z(x, \omega)$ is the time Fourier transform of the particle velocity $v_z(x, t)$, $V_z(x, \omega) = F_t\{v_z(x, t)\}$, and ω_0 is the angular frequency $\omega_0 = 2\pi f_0$. From (12) we can see that the CSM can be directly estimated as follows:

$$\begin{aligned} \mu(x) &= \Re \left\{ \frac{-\rho \omega_0^2 V_z(x, \omega_0)}{\nabla^2 V_z(x, \omega_0)} \right\} \\ \eta(x) &= \Im \left\{ \frac{-\rho \omega_0^2 V_z(x, \omega_0)}{\nabla^2 V_z(x, \omega_0)} \right\}, \end{aligned} \tag{13}$$

where $V_z(x, \omega_0)$ at the specified angular frequency ω_0 is calculated by the Fourier transform; $\nabla^2 V_z(x, \omega_0)$ calculated using discrete Laplace function (The MathWorks) $del2(V_z(x, \omega_0))$ returns the discrete approximation of the Laplace differential operator applied to $V_z(x, \omega_0)$. Algorithm 1 summarizes the proposed algorithm for 2D-CSM estimation.

Algorithm 1: Estimates 2D-CSM

- Step 1. Establish a simulation scenario
- Step 2. Select stimulation frequency of $f_0 = 200\text{Hz}$.
- Step 3. Create shear wave propagation into the tissue.
- Step 4. Use Doppler ultrasound to measure particle velocity at location space 120×120
- Step 5. Extract the variance of noise and feed it into an LMS filter.
- Step 6. Use the LMS filter to improve SNR.
- Step 7. Use the Fast Fourier transform (FFT) to calculate the filtering signal.
- Step 8. Estimate each CSM in the space locations using (13).
- Step 9. Synthesize estimation data μ and η to create the 2D-CSM image.

The human body is a heterogeneous environment consisting of many organs and organizations with different structures. When the shear wave reaches two media interfaces with different acoustic impedance, one part will go in the original direction and continue to the next medium; the other part will be reflected. The reflectance more or less depends on the impedance difference between the two media and is characterized by a quantity called the reflectivity R, calculated using Equation (14).

$$R = (Z_2 - Z_1)^2 / (Z_2 + Z_1)^2 \tag{14}$$

Z_2 and Z_1 , the acoustic impedances of the environment, create the surface of separation

3. Results and Discussion

Establishing simulation scenario: 2D environment with size 120×120 mm, containing a circular tumor in the position (40 mm, 40 mm), tumor radius 15 mm (bio soft tissue area). $\mu_1 = 6000$ Pa and $\eta_1 = 1.2$ Pa.s are the elasticity and viscosity of the medium, while $\mu_2 = 8900$ Pa and $\eta_2 = 2.7$ Pa.s are the elasticity and viscosity of the tumor, respectively. $f = 200$ Hz, $\rho = 1000$ kg/m³ correspond to the needle's vibration frequency and the medium's mass density, the amplitude of vibrating needle 5 mm. The shear wave's particle velocity is estimated over the entire 2D medium plane at the positions 1 mm evenly spaced in both the X and Y axes. The biological soft tissue region is simulated, as shown in Figure 2. When shear waves meet the tumor's surface, suppose on the transmission line, a reflected shear wave will be generated. The incident and the reflected waves meet and change the particle's velocity, so the ultrasonic doppler measures this velocity change. Because the particle-wave velocity is the basis for estimating the CSM tissue's elasticity and viscosity according to Equation (13), a change in the particle-wave velocity affects the CSM estimate's accuracy.

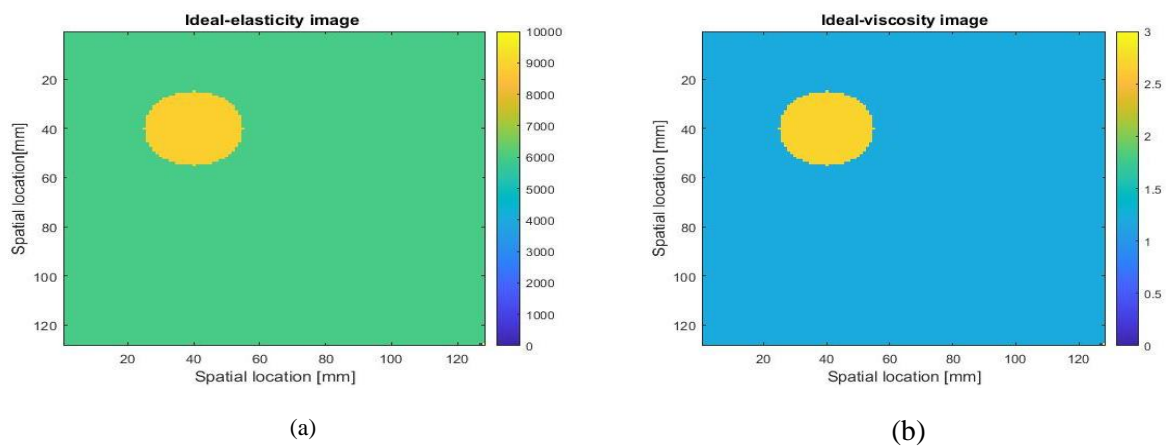


Figure 2. Image of elastic (a) and ideal viscous (b).

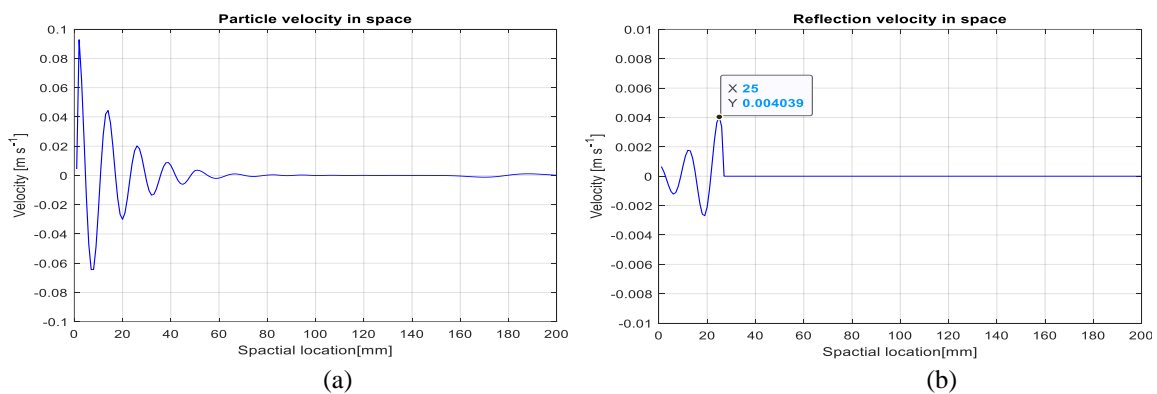


Figure 3. The velocity of particle wave (a) and reflected wave (b) in space.

The graph of particle velocity of shear waves is shown in Figure 3a. We see shear waves whose amplitude decreases with distance. Considering line 40 (the horizontal line passing through the tumor), the reflection phenomenon occurs at position $x = 25$. The graph of the reflected wave velocity is

depicted in Figure 3b. As a result, we measure the particle-wave velocity when there is no reflection and with reflection, as shown in Figures 4a and 4b.

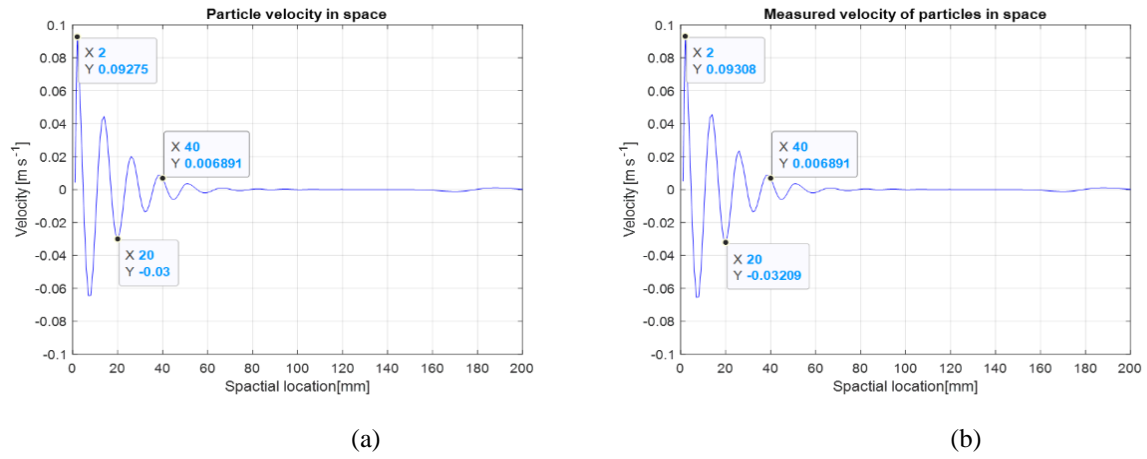


Figure 4. Wave-particle velocity without (a) and with (b) reflection.

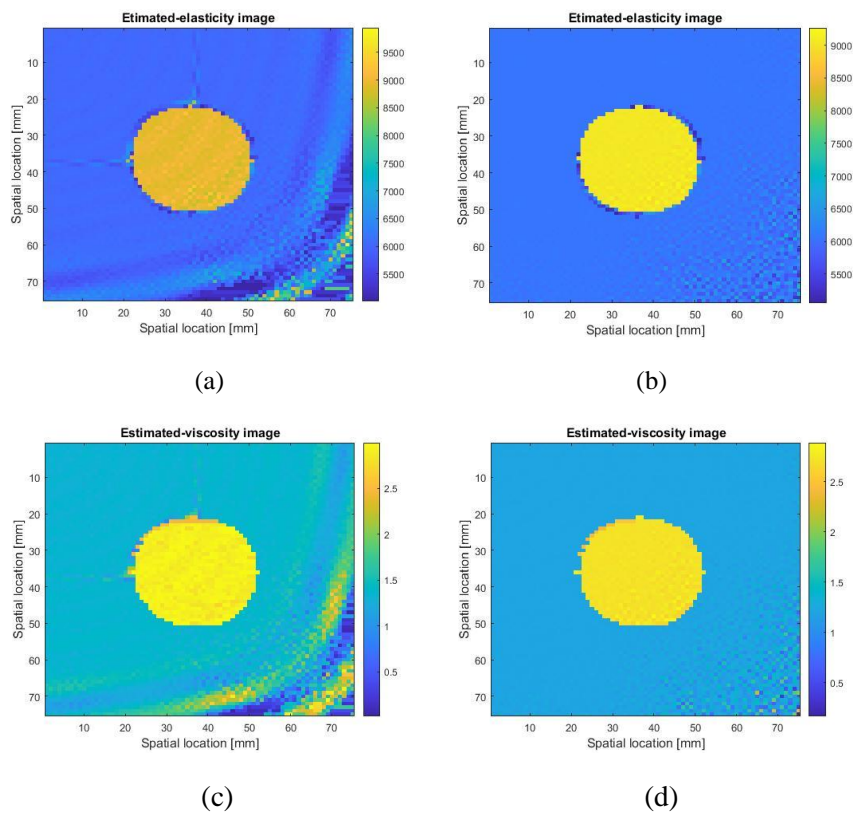


Figure 5. Estimation of elasticity with (a) and without (b) reflection, viscosity with (c) and without (d) reflection.

Table 1 presents the normalization error of CSM estimation with and without reflection. The quality of the reconstruction was degraded due to the effect of the reflection.

Table 1. Normalization error of CSM estimation with and without reflection

Normalization error	Without reflection	With reflection
ϵ_{μ}	0.0430	0.0754
ϵ_{η}	0.1412	0.2695

4. Conclusion

Two important parameters (elasticity and viscosity) in shear-wave ultrasound imaging were estimated to examine the tissue structure. The wave propagation is modeled using the FDTD method. An LMS filter is used to reduce the measurement noise. The algebraic Helmholtz inversion algorithm is used to estimate CSM directly. The 2D shear-wave images are reconstructed in the environment considering both the Gaussian noise and shear waves' reflection. The CSM estimation results were expressed in 2D images and quantitatively evaluated by normalization error when considering and not considering the effect of shear wave reflection. The results need to be verified by experimental data before being applied in biomedical imaging practice.

Acknowledgments

This work was supported by National Foundation for Science and Technology Development (NAFOSTED) under Grant 103.05-2020.13.

References

- [1] A. P. Sarvazyan, O. V. Rudenko, S. D. Swanson, J. B. Fowlkes, S. Y. Emelianov, Shear Wave Elasticity Imaging: A New Ultrasonic Technology of Medical Diagnostics, *Ultrasound in Medicine & Biology*, Vol. 24, No. 9, 1998, pp. 1419-1435, [https://doi.org/10.1016/S0301-5629\(98\)00110-0](https://doi.org/10.1016/S0301-5629(98)00110-0).
- [2] S. Chen, M. W. Urban, C. Pislaru, R. Kinnick, Y. Zheng, A. Yao, J. F. Greenleaf, Shearwave Dispersion Ultrasound Vibrometry (SDUV) for Measuring Tissue Elasticity and Viscosity. *IEEE Transactions on Ultrasonics, Ferroelectrics, and Frequency Control*, Vol.56, No.1, 2009, pp. 55-62, <https://doi.org/10.1109/TUFFC.2009.1005>.
- [3] M. Orescanin, M. F. Insana, Model-Based Complex Shear Modulus Reconstruction: A Bayesian Approach, *IEEE International Ultrasonics Symposium*, IEEE, 2010, pp. 61-64.
- [4] S. W. Hou, A. N. Merkle, J. S. Babb, R. McCabe, S. Gyftopoulos, R. S. Adler, Shear Wave Ultrasound Elastographic Evaluation of the Rotator Cuff Tendon, *Journal of Ultrasound in Medicine*, Vol. 36, No. 1, 2017, pp. 95-106, <https://doi.org/10.7863/ultra.15.07041>.
- [5] J. A. Sande, S. Verjee, S. Vinayak, F. Amersi, M. Ghesani, Ultrasound Shear Wave Elastography and Liver Fibrosis: A Prospective Multicenter Study, *World Journal of Hepatology*, Vol. 9, No. 1, 2017, pp. 38-47, <https://doi.org/10.4254/wjh.v9.i1.38>.
- [6] D. T. Tran, Y. Wang, L. T. Nguyen, M. N. Do, M. F. Insana, Complex Shear Modulus Estimation Using Maximum Likelihood Ensemble Filters, *4th International Conference on Biomedical Engineering in Vietnam*, Springer, 2013, pp. 313-316.

- [7] M. Orescanin, Y. Wang, M. F. Insana, 3-D FDTD Simulation of Shear Waves for Evaluation of Complex Modulus Imaging, *IEEE Transactions on Ultrasonics, Ferroelectrics, and Frequency Control*, Vol. 58, No. 2, 2011, pp. 389-398, <https://doi.org/10.1109/TUFFC.2011.1816>.
- [8] S. Papazoglou, U. Hamhaber, J. Braun, I. Sack, Algebraic Helmholtz Inversion in Planar Magnetic Resonance Elastography, *Physics in Medicine & Biology*, Vol. 53, No. 12, 2008, pp. 31-47, <https://doi.org/10.1088/0031-9155/53/12/005>.
- [9] L. Q. Hai, D. T. Tran, N. L. Trung, H. T. Huynh, M. N. Do, Simulation Study of 2D Viscoelastic Imaging of Soft Tissues Using the Extended Kalman Filter for Tumor Detection, *SIMULATION: Transactions of The Society for Modeling and Simulation International*, Vol. 96, No. 5, pp. 435-447, <https://doi.org/10.1177/0037549719873381>.
- [10] P. T. T. Ha, Q. H. Luong, V. D. Nguyen, D. T. Tran, H. T. Huynh, Two-Dimensional Complex Shear Modulus Imaging of Soft Tissues by Integration of Algebraic Helmholtz Inversion and LMS Filter Into Dealing with Noisy Data: A Simulation Study, *Mathematical Biosciences and Engineering*, 2020, Vol. 17, No. 1, pp. 404-417, <https://doi.org/10.3934/mbe.2020022>.
- [11] H. Duan, P. Chaemsaitong, X. Ju, S. Y. S. Ho, Q. Sun, Y. Y. Tai, Y. L. Tak, L. C. Poon, Shear-wave Sonoelastographic Assessment of Cervix in Pregnancy, *Acta Obstetrica Et Gynecologica Scandinavica*, Vol. 99, No. 11, 2020, pp. 1458-1468, <https://doi.org/10.1111/aogs.13874>.
- [12] V. J. Schrier, J. Lin, A. Gregory, A. R. Thoreson, A. Alizad, P. C. Amadio, M. Fatemi, Shear Wave Elastography of the Median Nerve: A Mechanical Study, *Muscle & Nerve*, Vol. 61, No. 6, 2020, pp. 826-833, <https://doi.org/10.1002/mus.26863>.